© 2015. Published by The Company of Biologists Ltd | Journal of Cell Science (2015) 128, 670–682 doi:10.1242/jcs.157115

RESEARCH ARTICLE

Regulation of Sec16 levels and dynamics links proliferation and secretion

Kerstin D. Tillmann[1,2], Veronika Reiterer[1], Francesco Baschieri[1,2], Julia Hoffmann[3], Valentina Millarte[1,2], Mark A. Hauser[1], Arnon Mazza[4], Nir Atias[4], Daniel F. Legler[1], Roded Sharan[4], Matthias Weiss[3,*] and Hesso Farhan[1,2,*]

ABSTRACT

We currently lack a broader mechanistic understanding of the integration of the early secretory pathway with other homeostatic processes such as cell growth. Here, we explore the possibility that Sec16A, a major constituent of endoplasmic reticulum exit sites (ERES), acts as an integrator of growth factor signaling. Surprisingly, we find that Sec16A is a short-lived protein that is regulated by growth factors in a manner dependent on Egr family transcription factors. We hypothesize that Sec16A acts as a central node in a coherent feed-forward loop that detects persistent growth factor stimuli to increase ERES number. Consistent with this notion, Sec16A is also regulated by short-term growth factor treatment that leads to increased turnover of Sec16A at ERES. Finally, we demonstrate that Sec16A depletion reduces proliferation, whereas its overexpression increases proliferation. Together with our finding that growth factors regulate Sec16A levels and its dynamics on ERES, we propose that this protein acts as an integrator linking growth factor signaling and secretion. This provides a mechanistic basis for the previously proposed link between secretion and proliferation.

KEY WORDS: ER exit sites, Sec16, Signaling

INTRODUCTION

Understanding cell homeostasis with respect to transcriptional, translational and post-translational networks is a major challenge in cell and developmental biology. Intense research in the past decades has fostered our understanding of a number of regulatory circuits, such as those that orchestrate cell polarity or cell proliferation. By contrast, in the field of membrane traffic, a comprehensive understanding of the integration of membrane traffic with other cellular processes such as growth and proliferation is still fragmentary. In addition, little is known about how external cues like growth factors regulate the functional organization of the early secretory pathway.

Export from the endoplasmic reticulum (ER) occurs on ribosome-free regions of the rough ER called ER exit sites (ERES), where COPII vesicles form and shuttle nascent cargo proteins to downstream sites of the secretory pathway (Budnik and Stephens,2009; Lee et al., 2004; Zanetti et al., 2012). Sec16A (hereafter called Sec16) plays an important role in ERES homeostasis as it interacts with several COPII components and regulates their function (Bhattacharyya and Glick, 2007; Connerly et al., 2005; Farhan et al., 2008; Ivan et al., 2008; Supek et al., 2002; Watson et al., 2006; Espenshade et al., 1995; Gimeno et al., 1996; Whittle and Schwartz, 2010; Kung et al., 2012). Various post-translational modifications, such as phosphorylation (Farhan et al., 2010; Koreishi et al., 2013; Lord et al., 2011; Sharpe et al., 2011), ubiquitylation (Jin et al., 2012) or glycosylation (Dudognon et al., 2004), were reported to modulate ER export, but the molecular details and functional consequences of this regulation remain to be established. Several questions remain unanswered: how does phosphorylation of Sec16 (Farhan et al., 2010) lead to changes in ERES? What dynamic and molecular changes are associated with Sec16 phosphorylation? Is the biogenesis of ERES by growth factor signaling solely contingent on Sec16 or does it involve COPII components? The answers to these questions are important to obtain a full and integrative view of the regulation of the secretory pathway. Besides the regulation of the ER export machinery at the post-translational level, we need to gain knowledge on whether and how regulation of protein abundance (for instance by transcription factors) is relevant for the organization of the early secretory pathway.

Candidates for the latter are members of the early growth response (Egr) transcription factor family that are known to mediate transcriptional responses downstream of several stimuli that induce the Ras–MAPK signaling pathway. Proteins of the Egr family, which comprises four members, exhibit a low basal expression level, but are rapidly (1–2 h) induced by MAPK signaling and bind to a GCGG/TGGGCG consensus sequence in the promoter of target genes. Being early responsive genes downstream of mitogenic signals, Egr family members are known to play a role in controlling cell growth, proliferation and differentiation (Sukhatme, 1990; Fowler et al., 2011).

In the current work, we show that growth factors modulate Sec16 protein levels and dynamics. We propose that Sec16 acts as part of a coherent feed-forward loop, which integrates secretion and growth factor signaling.

RESULTS

Sec16 integrates growth factor signaling at the level of ERES

In order to determine the role of Sec16 in integrating growth factor signaling, we first determined whether the response of ERES to growth factor depletion requires Sec16. Therefore, we serum-starved HeLa cells for 6 h, which resulted in a robust

[1]Biotechnology Institute Thurgau (BITg) at the University of Konstanz, Unterseestrasse 47, CH-8280 Kreuzlingen, Switzerland. [2]University of Konstanz, Universitätsstrasse 10, Konstanz 78464, Germany. [3]Experimental Physics I, University of Bayreuth, Bayreuth 95440, Germany. [4]Blavatnik School of Computer Science, Tel Aviv University, Tel-Aviv 69978, Israel.

*Authors for correspondence (matthias.weiss@uni-bayreuth.de; hesso.farhan@uni-konstanz.de)

Received 23 May 2014; Accepted 10 December 2014

Journal of Cell Science

Journal of Cell Science (2015) 128, 670–682 doi:10.1242/jcs.157115

reduction in the number of ERES (labeled by Sec31 immunofluorescence). Importantly, knockdown of Sec16 inhibited this response, showing that the reduction in the number of ERES by growth factor starvation causally depends on Sec16 (Fig. 1A). However, this observation raises the question of whether any condition that reduces ERES number renders the cells unresponsive to changes in growth factor levels. Therefore, we performed knockdown experiments with four kinases (NME5, NME6, NME7 and PIP5K1C), which we previously identified to reduce ERES number (Farhan et al., 2010). Knockdown cells displayed on average ~25% reduction in ERES number but the levels of Sec16 were not affected (supplementary material Fig. S1A,B), indicating that the reduction in ERES number occurs through a mechanism that is independent of Sec16 protein levels. In accordance with the interpretation that growth factors signal to ERES through Sec16, none of these four knockdowns affected the ability of ERES to respond to changes in growth factor status (supplementary material Fig. S1A). We also performed a knockdown of Sar1A, the GTPase that initiates the COPII assembly cascade. Depletion of Sar1A reduced the number of ERES and rendered them insensitive to the amount of growth factors (supplementary material Fig. S1), similar to what we

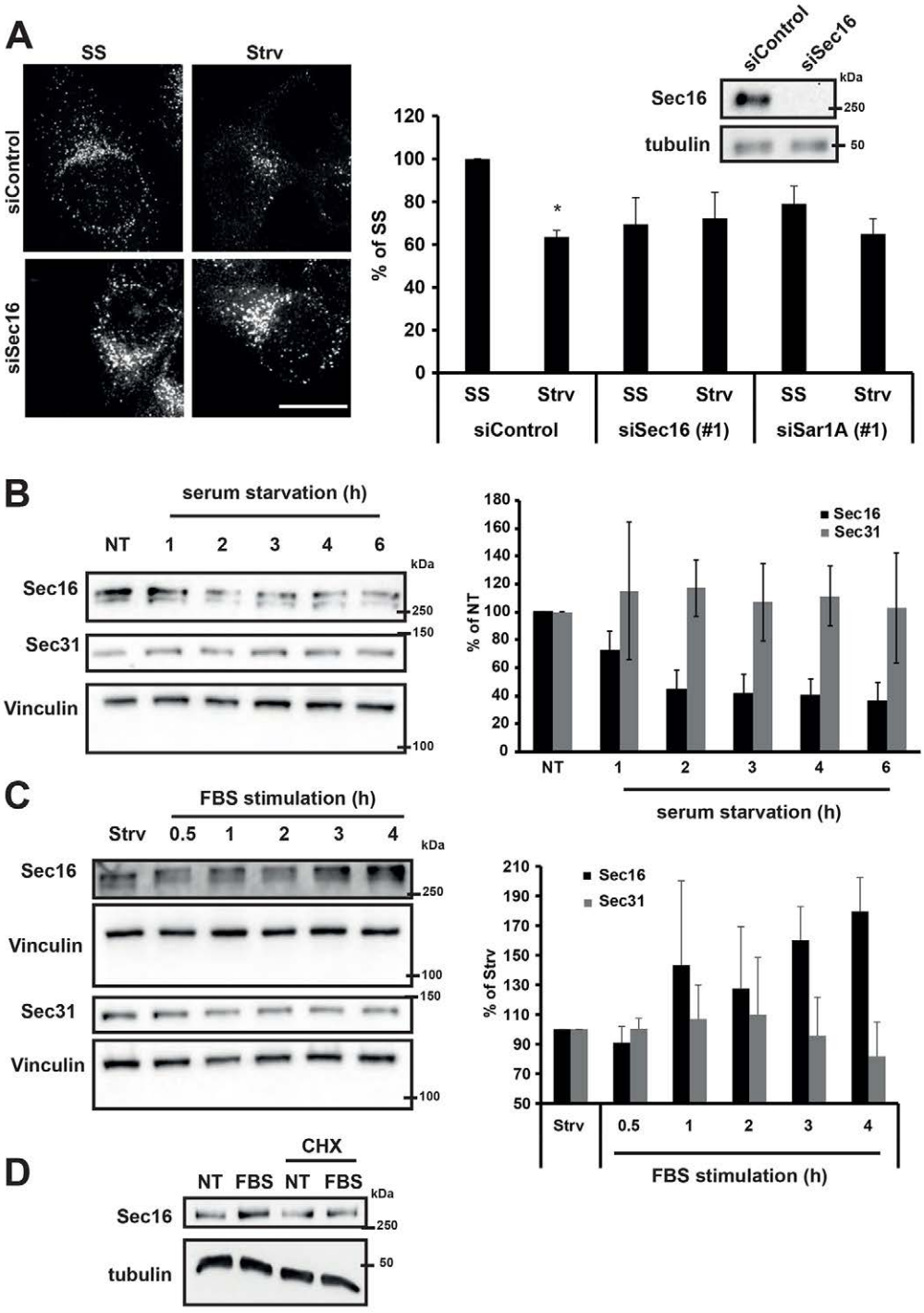

Fig. 1. Growth factor levels regulate Sec16 expression levels. (A) HeLa cells were transfected with control siRNA (siControl) or siRNA against Sec16 (siSec16). After 72 h, cells were left in steady state (SS) or were serum starved (Strv) for 6 h followed by fixation, Sec31 immunostaining and confocal microscopy. The right panel shows an immunoblot demonstrating the efficiency of Sec16 knockdown and a graphic representation of the number of ERES per cell presented as a percent of control in steady state. This value amounts to 156.4±32 ERES. Results show the mean±s.d. from three independent experiments with >50 cells per experiment. *$P<0.01$ (paired two-tailed Student's *t*-test). Scale bar: 10 µm. (B) HeLa cells were either left untreated (NT) or serum-starved for the indicated times. Cell lysates were immunoblotted for the indicated proteins. The left panel shows a representative experiment and the right panel shows an evaluation of three independent experiments on Sec16 (black bars) and Sec31 (gray bars) levels. The data show the mean±s.d. and are represented as a percentage of the untreated control. (C) HeLa cells were serum-starved for 4 h or treated with 10% FBS as indicated. Cell lysates were immunoblotted for the indicated proteins. The left panel shows a representative experiment and the right panel shows an evaluation of three independent experiments depicting expression of Sec16 (black bars) and Sec31 (gray bars). The data show the mean±s.d. and are presented as a percentage of the serum-starved condition. (D) HeLa cells were either left untreated or were stimulated with 10% FBS for 4 h. CHX, cycloheximide treatment for 30 min prior to FBS stimulation. Cell lysates were immunoblotted for the indicated proteins.

Journal of Cell Science

Journal of Cell Science (2015) 128, 670–682 doi:10.1242/jcs.157115

observed in Sec16-depleted cells. Therefore, the ability of ERES to respond to growth factors required the presence of Sec16 and COPII.

Absence of growth factor signaling decreases Sec16 synthesis

To determine whether the absence of growth factors alters ERES by changing the levels of Sec16, we serum-starved cells and observed a reduction in Sec16 levels with a halftime of about 2–3 h (Fig. 1B). By contrast, Sec31 levels remained largely unchanged. Adding back growth factors (i.e. treatment with serum) increased Sec16 levels after ~3–4 h of stimulation (Fig. 1C). This effect was dependent on *de novo* protein synthesis because it was absent in cells treated with cycloheximide (Fig. 1D). Thus, Sec16 levels are controlled by growth factor signaling.

The results shown above imply that Sec16 is a short-lived protein. Indeed, chasing Sec16 levels after blocking translation revealed that Sec16 has a half-life of ~2–3 h (Fig. 2A). Serum starvation likewise resulted in a decrease in Sec16 levels (Fig. 2B). The decrease in Sec16 levels can be explained either by an increase in protein degradation, by a reduction in the rate of synthesis or by a combination of both. First, we determined whether Sec16 is, in principle, degraded by the proteasome, which was the case, given that treatment with MG132 increased Sec16 levels and prevented its decay in cycloheximide-treated cells. If an increased degradation is the main cause for the reduction in Sec16 levels under serum starvation, then we might expect that the decay kinetics under serum starvation are higher than under cycloheximide treatment. This was not the case (Fig. 2B). Therefore, we conclude that, although the degradation of Sec16 is in principle mediated by the proteasome, the decay in Sec16 levels under serum starvation are not caused by an increase in the rate of proteasomal degradation. Thus, we next tested whether growth factor signaling regulates Sec16 synthesis.

Control of Sec16 synthesis could, in principle, occur through storage of the mRNA in stress granules, where it is trapped and prevented from undergoing translation. However, we did not observe any evidence for the formation of stress granules as determined using staining for VCP, which labels such structures (data not shown; Buchan et al., 2013). Another possibility is that growth-factor-sensitive transcription factors control Sec16 levels. To test this, we bioinformatically analyzed a 500-bp region upstream of the transcription start site of the Sec16 gene. This region was scanned for the presence of transcription factor binding sites, which revealed >90 candidates (supplementary material Table S1). These transcription factors were ranked based on the number of potential binding sites in the Sec16 promoter and by the sum of their distance (in a protein–protein interaction network) to two growth factor receptors, namely EGFR and IGFR. This approach revealed Egr family transcription factors as the most likely candidates (Fig. 3A). Individual knockdown of Egr1 or Egr3 did not reduce Sec16 expression (data not shown) but co-knockdown of Egr1 and Egr3 resulted in a clear reduction in Sec16 levels (Fig. 3B,C). Next, we determined whether the induction of Sec16 levels by mitogen treatment is dependent on Egr1 or Egr3. Treatment of cells with serum for 4 h resulted in a robust induction of Sec16 protein expression, and this response was completely ablated in Egr1 or Egr3 knockdown cells (Fig. 3D). Of note, although single knockdowns of Egr1 or Egr3 did not per se reduce Sec16 levels, they nevertheless prevented Sec16 induction upon serum treatment. Egr

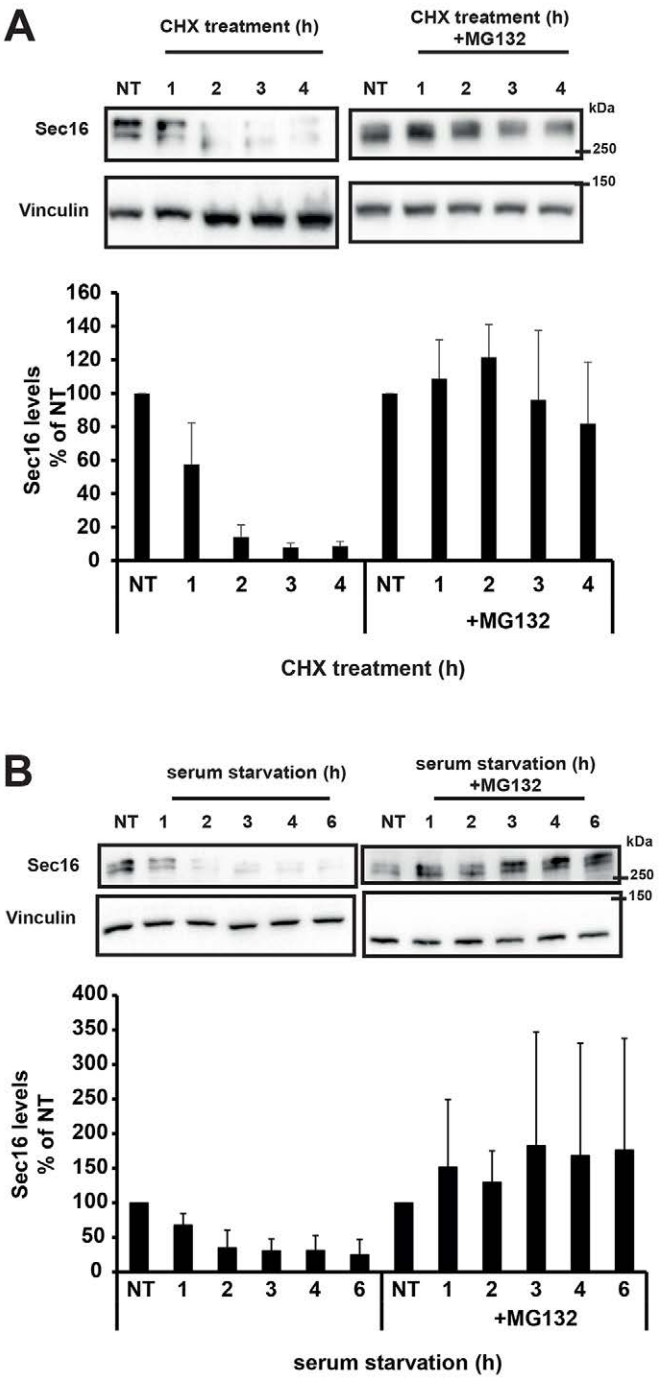

Fig. 2. Sec16 is a short-lived protein that is rescued by proteasomal inhibition. (A) HeLa cells were either left untreated (NT) or were treated with cycloheximide (CHX) as indicated. Alternatively, cells were pre-treated with MG132 for 30 min prior to cycloheximide addition (+MG132). Cells were lysed and immunoblotted against the indicated proteins. The upper panel shows a representative experiment and the lower panel shows an evaluation of three independent experiments. Values show the mean±s.d. and are presented as a percentage of the untreated control. (B) HeLa cells were either left untreated or were serum-starved for the indicated times. Alternatively, cells were pre-treated with MG132 for 30 min prior to serum-starvation (+MG132). Cells were lysed, and the lysates were subjected to SDS-PAGE and immunoblotting against the indicated proteins. The upper panel shows a representative experiment and the lower panel shows an evaluation of three independent experiments depicting the expression of Sec16. Values show the mean±s.d. and are represented as a percentage of the untreated control.

Journal of Cell Science (2015) 128, 670–682 doi:10.1242/jcs.157115

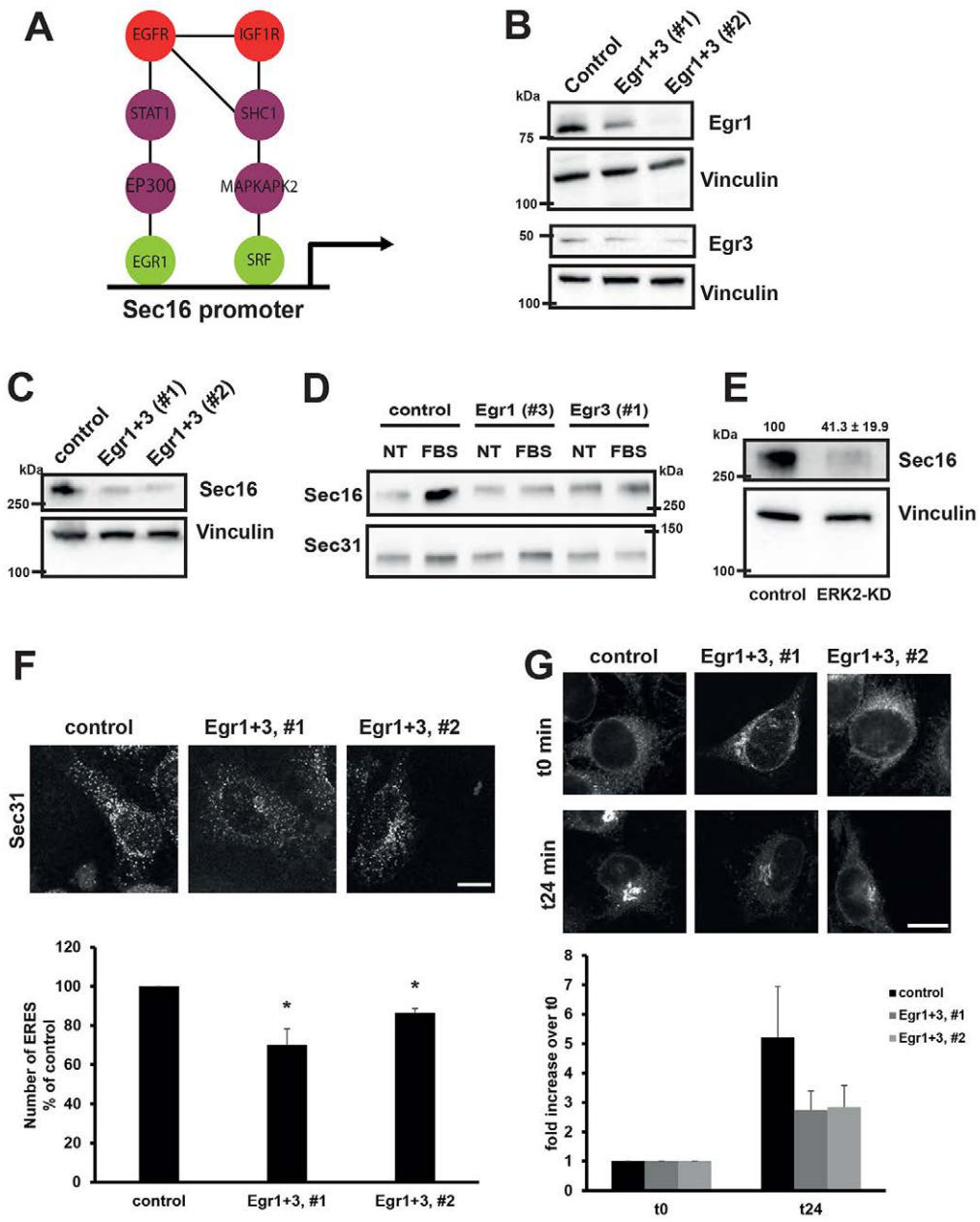

Fig. 3. Egr family transcription factors regulate Sec16 expression. (A) Schematic representation of the results of our bioinformatic analysis as described in the text. Green nodes are transcription factors predicted to bind to the Sec16 promoter. Red nodes are the two growth factor receptors to which the transcription factors were linked through intermediate proteins (purple nodes). Lines show experimentally documented physical interactions. (B,C) HeLa cells were transfected with non-targeting siRNA (Control) or with two different combinations of siRNA against Egr1 and Egr3 (Egr1+3). After 72 h, cells were lysed and immunoblotted for the indicated proteins. (D) HeLa cells were transfected with non-targeting siRNA or with siRNA against Egr1 or Egr3. After 72 h, cells were either harvested directly (NT) or treated with 10% FBS (FBS) for 4 h prior to lysis and immunoblotting as indicated. (E) HeLa cells were transfected with non-targeting siRNA or with siRNA against ERK2 (ERK2-KD). Cells were lysed after 72 h and immunoblotted for the indicated proteins. (F) HeLa cells were transfected with control siRNA or siRNA against Egr1 and Egr3. After 72 h, cells were fixed, stained for Sec31 and imaged using confocal microscopy. ERES were counted using ImageJ. The results are presented as a percentage of the control and this value amounts to 244.25±13.62 ERES. The results show the mean±s.d. from three independent experiments where ≥50 cells were evaluated per experiment. *$P<0.05$ (ANOVA with Tukey's post hoc test). (G) HeLa cells stably expressing GFP-tagged mannosidaseII RUSH construct were transfected with control siRNA or siRNA against Egr1 and Egr3. After 72 h, ManII–GFP was released by adding biotin, and cells were fixed at the indicated subsequent time-points. The lower panel shows a bar graph of fluorescence intensity at the Golgi area, normalized to ER fluorescence, presented as the fold increase over fluorescence intensity at *t*0. This value amounts to 9.52±3.6 in control cells and 9.27±3 or 12.32±2.6 in clones #1 and #2 in Egr1+3 knockdown cells, respectively. The results show the mean±s.d. from three independent experiments with ≥50 cells per experiment. Scale bars: 10 μm.

transcription factors are activated downstream of ERK2 (also known as MAPK1) signaling, and accordingly, depletion of this kinase reduced Sec16 levels (Fig. 3E).

In accordance with their ability to regulate Sec16 levels, co-depletion of Egr1 and Egr3 resulted in a reduction in the number of ERES (Fig. 3F) and the extent of this reduction was

Journal of Cell Science

Journal of Cell Science (2015) 128, 670–682 doi:10.1242/jcs.157115

comparable to what we have previously observed in Sec16 knockdown cells (Fig. 1; Farhan et al., 2010). We used the recently described retention using selective hooks (RUSH) system (Boncompain et al., 2012) to test for effects on ER–Golgi trafficking. This system relies on ER retention of secretory cargo using streptavidin-based retention. Treatment of the cells with biotin relieves retention and liberates the cargo that enters the secretory pathway. We used cells stably expressing GFP-tagged mannosidase II (ManII-RUSH). Double knockdown of Egr1 and Egr3 led to a marked delay in the arrival of ManII-RUSH from the ER to the Golgi (Fig. 3G), and the effect was comparable to that observed in cells depleted of Sec16 (supplementary material Fig. S2A). No effect of Egr1 and Egr3 double knockdown on Golgi to plasma membrane trafficking was observed (supplementary material Fig. S2B), thus excluding pleiotropic effects on the secretory pathway.

Cargo load has previously been shown to affect ERES number (Farhan et al., 2008; Guo and Linstedt, 2006), and therefore we determined whether the observed reduction in the number of ERES in Egr1 and Egr3 double knockdown cells is due to a change in Sec16 levels or due to alterations in the synthesis of secretory proteins. To test this, we used the hepatic cell line HepG2, which is a stronger secretory cell than HeLa cells. Egr1 and Egr3 double knockdown decreased the number of ERES (Fig. 4A). However, silencing Egr1 and Egr3 did not affect the levels of α1 antitrypsin (AAT1) (Fig. 4B), a major secretory protein in HepG2 cells (Nyfeler et al., 2008; Reiterer et al., 2010). A similar result was obtained with albumin, the most prevalent cargo in hepatocytes (Fig. 4C). Therefore, it is unlikely that Egr1 and Egr3 double knockdown reduces secretory cargo load.

Sec16 as part of a coherent feed-forward loop

Our results so far have revealed that growth factor signaling regulates Sec16 transcription, resulting in an increase in Sec16 levels on a timescale of 2–3 h after growth factor stimulation. In addition, growth factor signaling pathways are expected to induce translation, thereby increasing secretory cargo load. This scenario is reminiscent of a coherent feed-forward loop (CFFL; Fig. 5A) (Lim et al., 2013; Shen-Orr et al., 2002). In a CFFL, an input node (growth factors) triggers a central node (Sec16) that subsequently triggers an output node (secretion or ERES number). CFFLs are typically found as part of persistence detectors, which ensure that transient stimuli that are able to trigger the central node do not affect the output node to any appreciable extent. Only a prolonged (i.e. a persistent) stimulus is able to trigger the output node. A CFFL necessitates the presence of a fast connection between input and central node (i.e. between growth factors and Sec16). The connection ought to be considerably

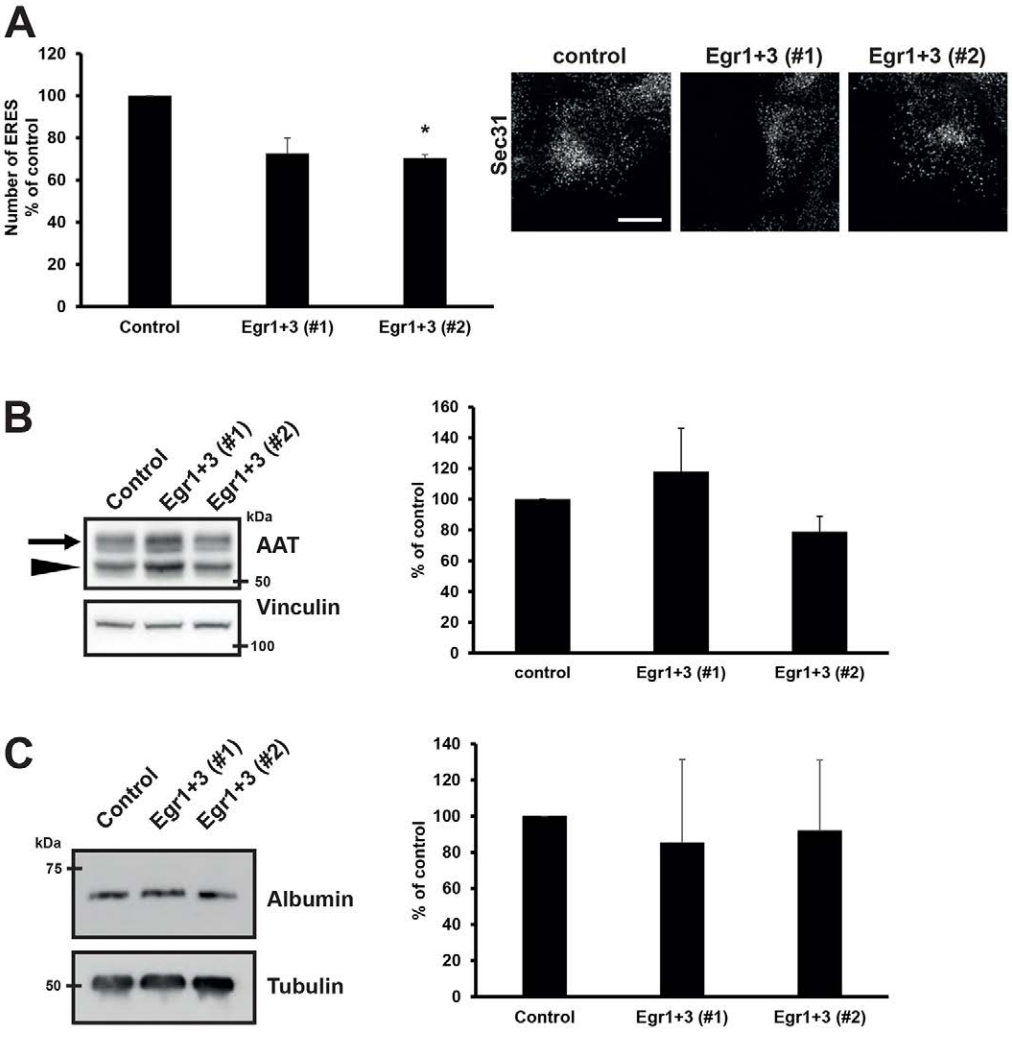

Fig. 4. The decrease in ERES number after loss of Egr1 and Egr3 is independent of cargo load in HepG2 cells. (A) HepG2 cells were transfected with control siRNA (control) or siRNA against Egr1 and Egr3 (Egr1+3). After 72 h, cells were fixed and stained for Sec31, and images were acquired by confocal microscopy. The left panel shows a graphic representation of the number of ERES per cell. The results are presented as a percentage of the control to account for inter-assay variance. This value amounts to 314±51 ERES. The results show the mean±s.d. from three independent experiments where ≥50 cells were evaluated per experiment. *$P<0.05$ (ANOVA with Tukey's post hoc test). Scale bar: 10 μm. (B,C) HepG2 cells were transfected with non-targeting siRNA or with siRNA against Egr1 and Egr3. After 72 h, cells were lysed and immunoblotted for α1-antitrypsin (AAT) in B or for albumin in C. The left panels show representative experiments and the right panels show evaluation of three independent experiments. Arrow, complex glycosylated AAT1; arrowhead, core glycosylated AAT1. Values show the mean±s.d. and are represented as a percentage of the control.

Journal of Cell Science (2015) 128, 670–682 doi:10.1242/jcs.157115

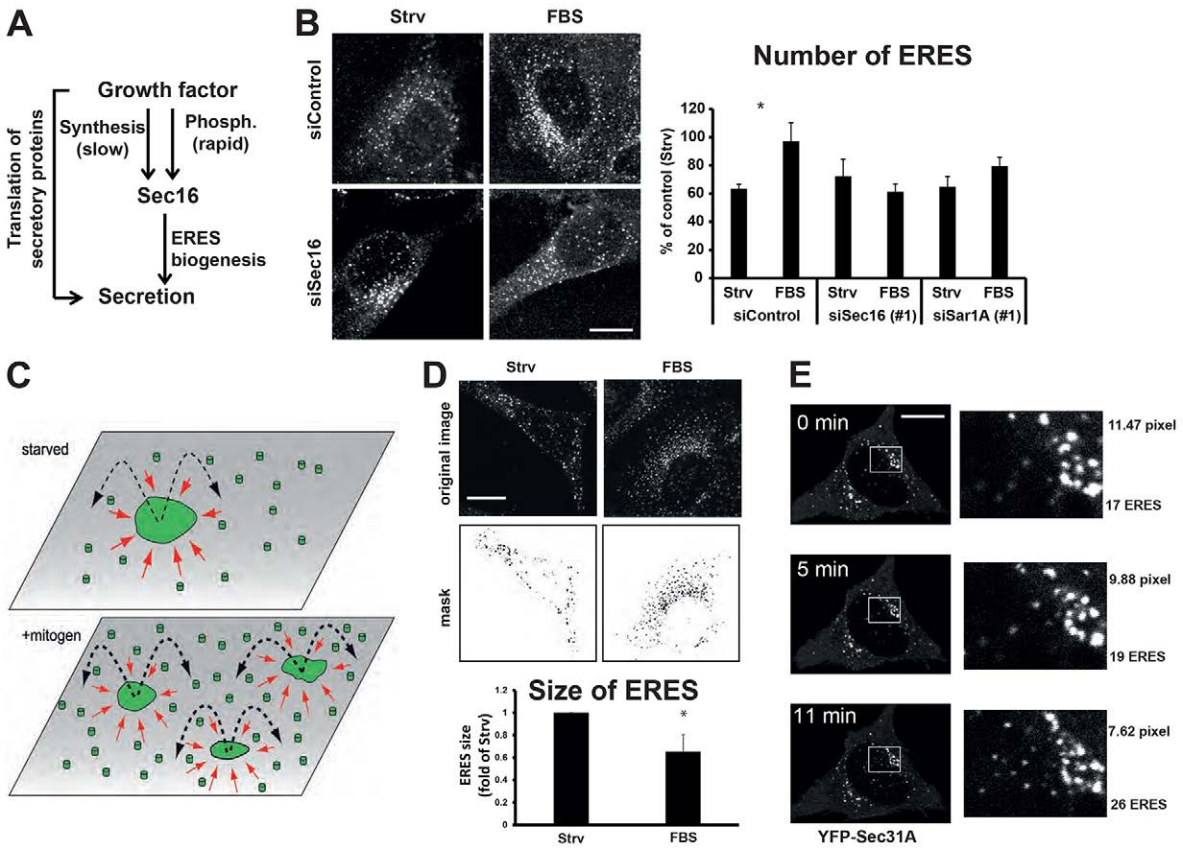

Fig. 5. Fast response of Sec16 to growth factors. (A) Schematic representation of the proposed coherent feed-forward loop. Phosph., phosphorylation. (B) HeLa cells were transfected with control siRNA (siControl) or siRNA against Sec16 (siSec16). After 72 h, cells were serum starved (Strv) for 6 h and fixed, or followed by 10% FBS treatment for 15 min (FBS) and fixation. Cells were stained for Sec31, and imaged by confocal microscopy. The right panel shows a graphic representation of the number of ERES per cell. Results are presented as a percentage of control (Strv) to account for interassay variance. The results show the mean±s.d. from three independent experiments where ≥50 cells were evaluated per experiment. *P<0.01 (paired two-tailed Student's t-test). (C) Schematic representation of the results of our mathematical modeling. In starved cells, Sec16 rarely leaves the ERES (thin black dashed arrows). Sec16 that escapes the ERES will rebind to and diffuse on ER membranes, where it is captured by existing ERES (red arrows). In mitogen-treated cells, dissociation is enhanced (thick black dashed arrows), and rebinding Sec16 molecules can form local assemblies on ER membranes that attract even more Sec16, thereby growing new ERES. (D) HeLa cells were serum starved for 4 h (Strv) and stimulated with 10% FBS for 15 min (FBS) followed by fixation immunostaining and confocal microscopy. The upper panel shows representative images of ERES as well as masks of counted particles as appearing for analysis. The lower panel shows a graphic representation of ERES size presented as the fold change compared to Strv. This value amounts to 96.9±19.2 pixels/ERES (~9.8×9.8 pixels or 462×462 nm for each ERES). The results show the mean±s.d. from three independent experiments with ≥10 cells per experiment. *P<0.05 (paired Student's t-test). (E) HeLa cells expressing YFP–Sec31A were serum starved for 4 h. Live imaging was started upon addition of 10% FBS and an image was acquired every 60 seconds. Stills are shown of the indicated time-points. The right panels are magnified areas and the numbers to the right are the mean ERES size (in pixels) and their number within the displayed region. Scale bars: 10 μm.

faster than between input and output nodes (i.e. between growth factors and secretion). We next tested whether and how a brief growth factor treatment affected Sec16 and ERES organization.

Growth factor treatment increases ERES number and alters Sec16 dynamics

We serum-starved cells, which results in a decrease in ERES number (Fig. 1A), and briefly (10–15 min) treated them with fetal bovine serum (FBS). We observed a rapid increase in ERES number, which was not the case in Sec16-depleted cells (Fig. 5B). This rapid response was dependent on ERK2 (supplementary material Fig. S1D,E) and is unlikely to be mediated by induction of Sec16 levels, because Sec16 levels did not change in the first 30 min of treatment (Fig. 1).

To gain more detailed insights into the mechanism that underlies the observed increase in ERES number, we adapted a previously reported simulation approach for the self-assembly of ERES (Heinzer et al., 2008). In agreement with experimental observations, our simulation revealed a quasi-crystalline arrangement of ERES with a fairly uniform size and a comparatively low density of Sec16 or COPII proteins on ER membranes between ERES. The steady state of ERES formation therefore can be described by an unmixing scenario of the Flory–Huggins type (Gedde, 1995). Analogous to a domain formation of small amphipathic polymers in water, Sec16 and/or COPII show a dynamic segregation into patchy domains on ER membranes (the ERES). However, in contrast to a standard Flory–Huggins scenario, Sec16 and/or COPII have finite residence times on ER membranes, i.e. they dissociate on average with rate Γ from ER membranes. Extending the Flory–Huggins scenario to include this aspect allowed us to analytically predict the steady-state number and radius of ERES (N_{ERES} and R_{ERES}, respectively) as a function of the protein density, ϕ, and the dissociation rate of the proteins and diffusion coefficient (Γ and D, respectively):

Journal of Cell Science (2015) 128, 670–682 doi:10.1242/jcs.157115

$N_{ERES}=\Gamma L^2/D$ and $R_{ERES}=\sqrt{4\phi D/(\pi\Gamma)}$, where L^2 is the area of the ER membrane. The model predicts that increasing the dissociation constant of Sec16, Γ, increases the number of Sec16-positive ERES irrespective of the available protein amount, ϕ. However, this happens at the expense of ERES size, because the ERES radius depends inversely on the dissociation rate Γ. In other words, Sec16 molecules must be able to leave ERES faster on average to be able to nucleate new, but smaller, ERES at remote locations (Fig. 5C). This conjecture is supported by our experimental finding that a brief (15 min) stimulation of serum-starved cells with FBS led to a reduction in the mean size of ERES (Fig. 5D). Live imaging of YFP–Sec31A showed that a brief stimulation with FBS increased ERES number and reduced their size (Fig. 5E), which agrees with the findings in fixed cells (Fig. 5B,D).

To test the model, we performed fluorescence recovery after photobleaching (FRAP) of single ERES in HeLa cells expressing GFP–Sec16 (Fig. 6A). We evaluated FRAP curves of individual ERES by assuming a simple binding reaction, i.e. using a single-exponential recovery. Sec16 association/dissociation events are stochastic in nature, i.e. a considerable variation of fitting parameters between individual FRAP curves was anticipated. Therefore, averaging FRAP curves to obtain a smoothed 'master' curve might introduce serious artifacts like stretched-exponential or even power-law recoveries (see, for example, Lee et al., 2001 for a related discussion on the sum of exponentials). We therefore fitted curves individually and averaged the obtained fitting parameters. Curves from starved and mitogen-treated cells did not vary with respect to half-time of recovery (~10 s). However, the extent of the recovery varied. As compared to their pre-bleach fluorescence (set to unity), the mean extent of fluorescence recovery of ERES was larger and the mobile fraction was higher when cells had been stimulated with growth factors (Fig. 6B,G), which is in line with our previous observations (Farhan et al., 2010).

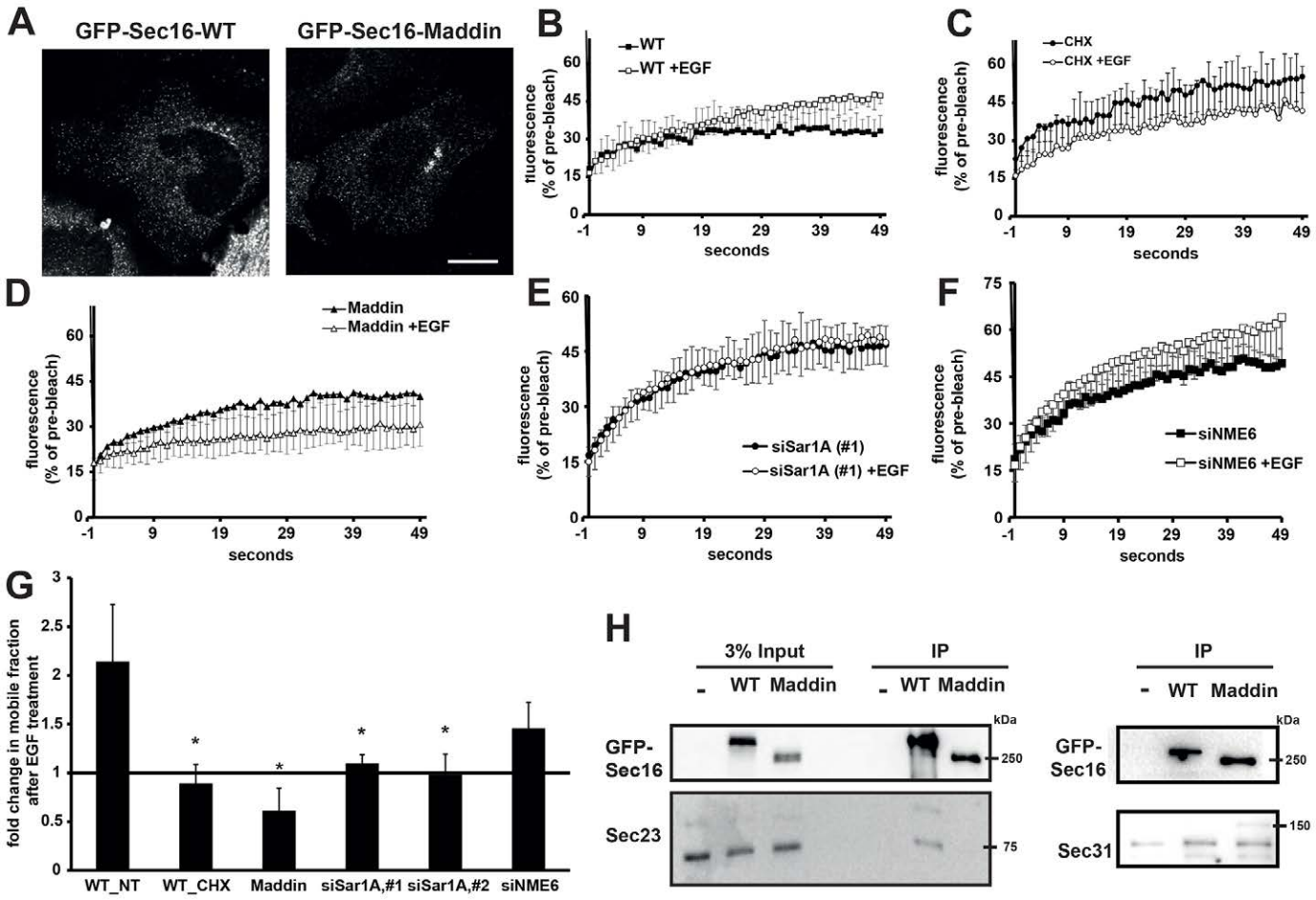

Fig. 6. FRAP analysis of Sec16 dynamics. (A) HeLa cells expressing GFP-tagged wild-type (WT) Sec16 (left) or Sec16-Maddin (right). Scale bar: 10 µm. (B) HeLa cells expressing wild-type GFP–Sec16. Cells were serum starved for 6 h. FRAP curves were recorded from the same coverslip before (black symbols) and after stimulation with 50 ng/ml EGF (+EGF; white symbols). FRAP curves are shown as the mean±s.d. of three independent experiments where at least five curves were recorded in each experiment. Fluorescence values were normalized to the pre-bleach intensity. (C) As for B, except that cells were pre-treated with 50 µg/ml cycloheximide (CHX) for 2 h before starting FRAP measurements. (D) Similar experimental setting as in B except that cells expressing GFP–Sec16-Maddin were used. (E,F) Similar to B, except that cells were transfected with siRNA against Sar1A (E) or NME6 (F) 72 h prior to FRAP measurement of wild-type GFP–Sec16. (G) Bar graph depicting the relative increase in mobile fractions, *q*, after treatment with EGF determined as indicated in Materials and Methods. WT_NT and WT_CHX indicate wild-type GFP–Sec16-expressing cells treated with solvent and cycloheximide, respectively. Values show the mean±s.d. from three independent experiments. *$P<0.05$ (ANOVA with Tukey's post hoc test). (H) HeLa cells expressing wild-type GFP–Sec16, GFP–Sec16-Maddin or GFP (-) were lysed and Sec16 was immunoprecipitated (IP) using GFP-trap beads. The immunoprecipitate was eluted from the beads and Sec16 was detected by immunoblotting. The same membrane was probed for the levels of Sec23A (Sec23) or Sec31.

If only a single pool of Sec16–GFP was present on ERES, one would expect either a full recovery ($q=1$) or no recovery at all ($q=0$) on the timescale of the FRAP experiment. Observing a recovery with a maximum value of q between zero and unity therefore requires the existence of a fast Sec16 pool that carries the observed recovery (relative amount q), and a slow Sec16 pool that does not contribute to the fluorescence recovery on the timescale of the FRAP experiment (relative amount $1-q$). Consequently, the arithmetically averaged dissociation rate of the entire Sec16 population is $\Gamma=q\Gamma_{fast}+(1-q)\Gamma_{slow}$. Observing an increase in q after growth factor stimulation therefore reports on a faster turnover kinetics of Sec16 on average (Γ is increased), whereas the half time of the recovery is only determined by Γ_{fast} (because the experiment takes much less time than $1/\Gamma_{slow}$). Yet, an increase in the mean dissociation rate Γ is exactly the prediction of the above model, and we therefore conclude that mobilization of Sec16 after mitogen stimulation is a factor that can drive formation of new ERES.

The number and size of ERES also depend on the diffusion constant of Sec16 on ER membranes, D. Thus, if our above rationale is to hold true, D must vary to a lesser extent than Γ between starved and mitogen-treated cells. To investigate this, we used fluorescence correlation spectroscopy (FCS) that allowed us to determine the diffusion constants of GFP–Sec16 in cytoplasm and on ER membranes (representative FCS curves are shown in supplementary material Fig. S3). We found that the diffusion constant of GFP–Sec16 in the cytoplasm agreed well with theoretical predictions for a soluble protein of ~280 kDa, irrespective of the treatment ($D\approx16$ μm^2/s). By contrast, the membrane-bound pool of Sec16 showed a reduction in the diffusion constant under serum starvation ($D\approx0.43$ μm^2/s) as compared with mitogen-treated cells ($D\approx0.65$ μm^2/s) and completely untreated cells ($D\approx0.62$ μm^2/s). This increase in diffusion upon mitogen treatment was in the range of ~50% and is thus smaller than the increase in the mobile fraction, which doubled after mitogen treatment (Fig. 6G). Most likely, the change in D and in Γ are linked: Γ is the weighted average of two dissociation constants, $\Gamma=q\Gamma_{fast}+(1-q)\Gamma_{slow}$, i.e. increasing Γ most likely means that the fast dissociation gains more weight (q increases). Given that Γ_{slow} is associated with a pool of Sec16 that is stuck in ERES (immobile on the timescale of our experiments), this ‘mobilization’ increases the amount of Sec16 molecules on ER regions between ERES. Increasing the pool of these free Sec16 molecules possibly leads to a more pronounced interaction with other ER-resident components, e.g. resulting in a transient formation of oligomeric structures, which consequently reduces the mean diffusion of Sec16 copies on ER patches between ERES. Nevertheless, Sec16 is regulated on the timescale of minutes, consistent with it being part of a CFFL. We next aimed at understanding how the mobilization of Sec16 generates more ERES.

Interaction with COPII modulates the turnover of Sec16 on ERES

We hypothesized that an interaction with COPII is responsible for the observed existence of a fast and a slow Sec16 pool and that thereby COPII plays a role in the ability of Sec16 to generate new ERES. If true, then decreasing the binding of COPII to ERES ought to affect the amount of fluorescence recovery, q, in FRAP experiments. As a first step, we treated cells with cycloheximide to reduce the protein load in the ER and, concomitantly, the association of COPII with ERES (Farhan et al., 2008; Forster et al., 2006). Although growth factor treatment in control cells led to an increase in Sec16 fluorescence recovery, the extent of recovery and the mobile fraction in cycloheximide-treated cells was the same for starved and mitogen-treated cells (Fig. 6C,G). To obtain further insight into the role of COPII, we performed FRAP experiments with a truncation mutant of Sec16 that lacks the last C-terminal 431 amino acids, which we called Sec16-Maddin. This mutant still contains the previously described ERK phosphorylation site Thr415 (Farhan et al., 2010) but it lacks the domain that was described to bind to Sec23A and Sec12 (Bhattacharyya and Glick, 2007; Montegna et al., 2012). Using co-immunoprecipitation, we confirmed that Sec16-Maddin fails to interact with Sec23A, but is still able to interact with Sec31 (Fig. 6H) as the Sec31-binding region has been previously mapped to the central region of Sec16 (Shaywitz et al., 1997). In FRAP experiments, treatment with growth factors did not increase but rather decreased the extent of recovery and mobile fraction of Sec16-Maddin (Fig. 6D,G). To further support the notion of the role of COPII, we depleted Sar1A and found EGF treatment did not change GFP–Sec16 mobility (Fig. 6E,G). Of note, depletion of Sar1A also affected the ability to form new ERES upon growth factor treatment (Fig. 1A; Fig. 5B). Depletion of NME6 lowered the number of ERES, but did not affect the ability of ERES to respond to growth factor treatment (supplementary material Fig. S1A) and also did not inhibit the increase in GFP–Sec16 mobility after EGF treatment (Fig. 6F,G). Thus, we propose that the COPII–Sec16 interplay might be important for the generation of new ERES after growth factor treatment.

Interaction with COPII is required for Sec16 to generate more ERES

To test the role of the Sec16–COPII interplay in the generation of more ERES after mitogen treatment, we determined the ERES number in cells expressing either wild-type GFP–Sec16 or Sec23-binding-deficient GFP–Sec16-Maddin. We only compared cells within a twofold range of fluorescence intensities to avoid inclusion of cells with a too high variability of GFP–Sec16 overexpression. Cells were fixed before and after treatment with serum for 15 min followed by confocal imaging. If the ability of Sec16 to interact with COPII is crucial to the generation of more ERES, then Sec16-Maddin should fail to respond to growth factor treatment. As observed with endogenous Sec16, growth factor treatment increased the number of ERES labeled with wild-type GFP–Sec16 (Fig. 7A). As a control, we tested whether the response required Sec16 phosphorylation of Thr415 and found this to be the case (Fig. 7A). ERES number also did not increase after mitogen stimulation in cells with GFP–Sec16-Maddin (Fig. 7A). Hence, Sec16–Sec23 seems to be relevant for the increase in the number of ERES upon mitogen treatment.

Finally, we tested the role of COPII using an *in vitro* recruitment assay. Semi-intact cells were extensively washed to strip off the majority of Sec16 and COPII from their endomembranes (Fig. 7B), followed by incubation with fresh cytosol, which led to recruitment of COPII and Sec16 and formation of new ERES. Reducing the load of secretory cargo by treatment with cycloheximide significantly reduced *de novo* formation of Sec16- and COPII-positive ERES (Fig. 7B–D). Taken together, our data underscore the necessity of Sec16 mobilization for ERES generation, and highlight that cooperation of Sec16 with COPII is required for the formation of new ERES after mitogen treatment.

Journal of Cell Science (2015) 128, 670–682 doi:10.1242/jcs.157115

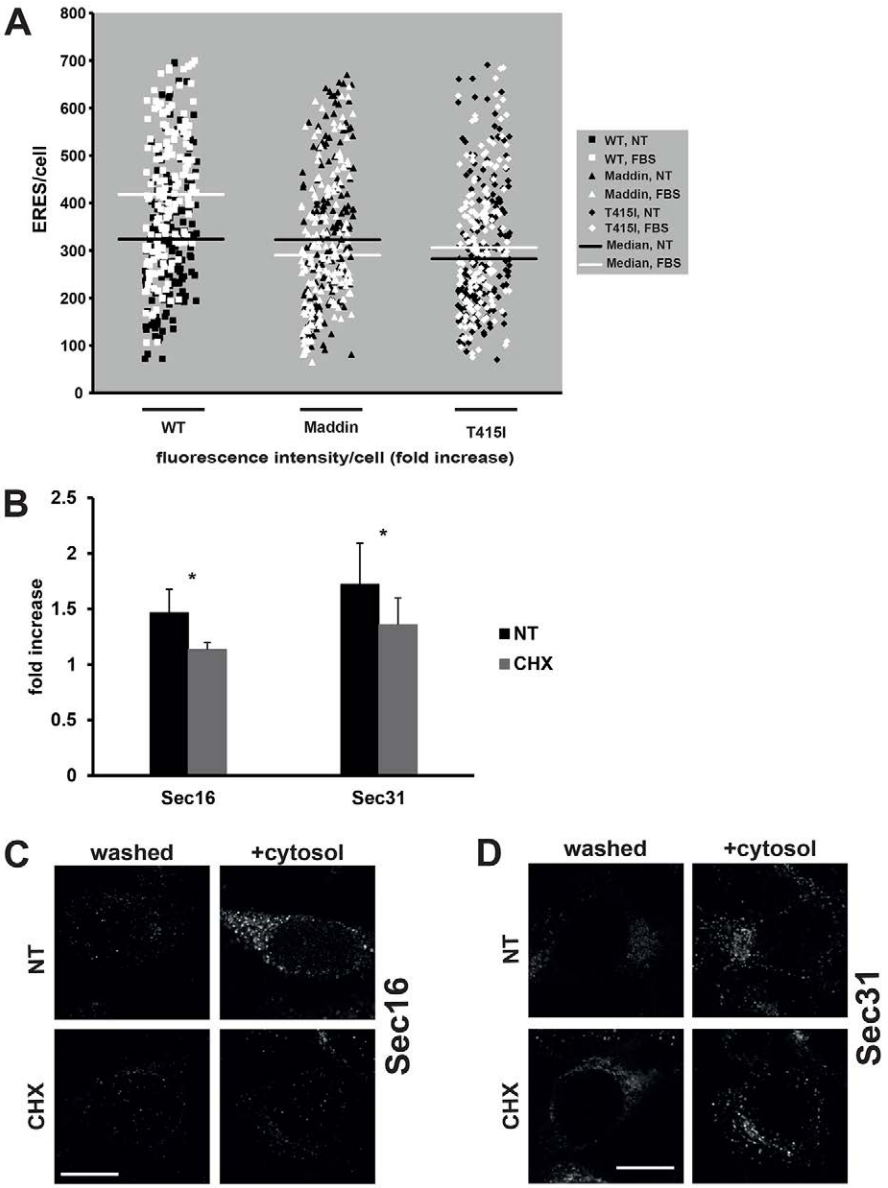

Fig. 7. Role of COPII and Sec16 in the biogenesis of ERES. (A) HeLa cells on glass coverslips were transfected with plasmid encoding wild-type GFP–Sec16 (WT), GFP–Sec16-Maddin (Maddin) or GFP–Sec16-T415I (T415I). After 24 h, cells were either fixed directly (NT) or treated with 10% FBS for 15 min (+FBS) followed by fixation. The number of Sec16-positive ERES was counted using ImageJ. Lines indicate the median number of ERES per cell from non-treated cells (black lines) or FBS-treated cells (white lines). (B–D) HeLa cells were plated on glass coverslips. After 24 h, cells were either not treated or treated with cycloheximide (CHX) for 2 h prior to the experiment. Cells were permeabilized and washed extensively to deplete COPII and Sec16. These cells were either fixed directly after washing (washed) or treated with cytosol harvested from HeLa cells (+cytosol) for 30 min at room temperature followed by fixation. Sec16 and Sec31 were detected using immunofluorescence. The numbers of Sec16-positive and Sec31-positive ERES were counted using ImageJ, and the bar graph in B shows the relative increase in Sec16-positive and Sec31-positive ERES under the condition '+cytosol' normalized to the condition 'washed'. Values show the mean±s.d. from four (Sec16) or three (Sec31) independent experiments. *$P<0.05$ (paired Student's *t*-test). Scale bars: 10 µm.

Cell proliferation is dependent on Sec16

Our results so far indicate that Sec16 integrates mitogenic signaling at the level of ERES. However, thus far, it is unclear whether Sec16 is relevant for the biological outcomes of mitogenic signaling, such as proliferation. In our previous work, we identified 64 kinases and phosphatases that, when depleted, reduce the number of ERES (Farhan et al., 2010). More recently, others have described 47 proteins that regulate ERES number (Simpson et al., 2012). We hypothesized that, if ER export is linked to the regulation of cell proliferation, then a network linking these hits (111) to Sec16 ought to be enriched in cellular processes related to cell proliferation. We therefore constructed an anchored network of these 111 hits with Sec16 as an anchor, using an algorithm described previously (Yosef et al., 2011). This anchored network was analyzed for enrichment of biological processes (GO term annotation). Indeed, this approach revealed several proliferation-related processes that were significantly enriched (Fig. 8A), suggesting a link between ER export and cell proliferation. To test this experimentally, we performed a Sec16 knockdown and measured the increase in cell number for 2 days. We found that depletion of Sec16 inhibited cell proliferation (Fig. 8B), and this effect was not attributed to an increase in apoptosis as assessed by determining caspase-3 cleavage (Fig. 8C). The Ras–ERK1/2 pathway is a well-known regulator of proliferation, and it is also known to induce Egr family members, which we experimentally verified (Fig. 8D). In line with our finding that Egr members control Sec16 levels, Ras overexpression also induced a threefold increase in Sec16 (Fig. 8D). We tested whether Sec16 is involved in the Egr-dependent control of proliferation. Silencing Egr1 and Egr3 together resulted in an inhibition of cell proliferation, which was overcome by overexpressing Sec16 (Fig. 8E). Overexpressing Sec16 significantly induced proliferation (Fig. 8E; supplementary material Fig. S4), indicating that Sec16 is necessary and sufficient for proliferation. We also overexpressed the Sec16-T415I mutant as well as Sec16-Maddin and determined the effect on proliferation. HeLa cells overexpressing these mutants proliferated more than GFP-expressing cells, but significantly less than cells expressing wild-type Sec16. Sec16 forms oligomers and Sec16 mutants are expected to oligomerize with

Journal of Cell Science (2015) 128, 670–682 doi:10.1242/jcs.157115

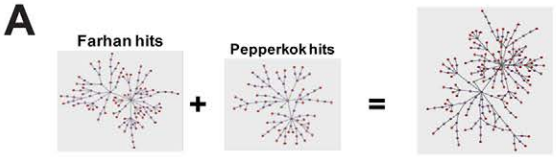

List of enriched biological processes related to cell proliferation

GO-ID	Description	corr p-val	Genes
42127	regulation of cell proliferation	3.90E-09	PRKCZ CAV1 CLU NFKBIA FOXO1 TNFRSF5 RPS6KB1 PTEN CTNNB1 CUL2 KRAS GAB2 CTGF PRKCA EGFR AR VHL SMAD4 TP53 RAF1 RB1 KDR CAPN1 MAPK1 SSTR2 NOTCH1 HIF1A HDAC1 NUP62 NME1 JUN VEGFA PDGFRA MDM2 HGS NGFR SST
8284	positive regulation of cell proliferation	3.70E-06	PRKCA EGFR PRKCZ CLU TNFRSF5 RPS6KB1 CTNNB1 KDR CAPN1 MAPK1 NOTCH1 HIF1A KRAS HDAC1 GAB2 CTGF NME1 JUN VEGFA PDGFRA MDM2 NGFR
8285	negative regulation of cell proliferation	1.39E-04	PRKCA AR CAV1 VHL SMAD4 TP53 RAF1 RB1 PTEN CTNNB1 CUL2 SSTR2 NUP62 NME1 JUN HGS SST
50678	regulation of epithelial cell proliferation	1.80E-04	EGFR AR NOTCH1 NME1 VEGFA PTEN KDR CTNNB1
82	G1/S transition of mitotic cell cycle	7.33E-05	EGFR CUL2 PIM1 RPS6KB1 RB1 RHOU CDC25A
45786	negative regulation of cell cycle	9.30E-04	KHDRBS1 EGFR CUL2 HDAC1 MAPK12 TP53 DGKZ NGFR RB1 CDK5
51726	regulation of cell cycle	1.37E-07	KHDRBS1 EGFR ROCK2 PIM1 TP53 RPS6KB1 RB1 CDK7 CDK5 PTEN CDC25A SIRT2 CSNK2A2 CUL2 FBXW7 APP HDAC1 MAPK12 CTGF JUN BUB1B MDM2 DGKZ NGFR

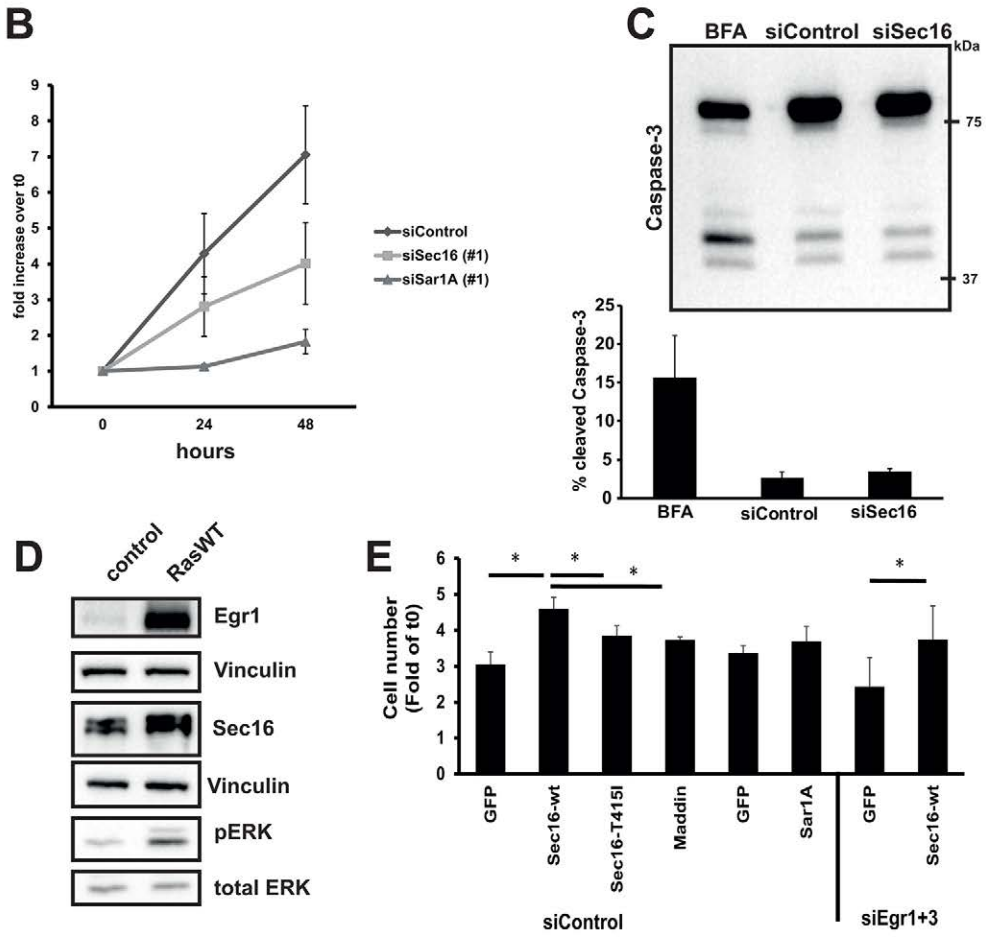

Fig. 8. Sec16 represents a link between the secretory pathway and cell proliferation. (A) The upper panel shows hits from previous screens (Farhan et al., 2010; Simpson et al., 2012) (Farhan hits and Pepperkok hits) that were also anchored to Sec16 and the networks were merged (right network). The lower panel shows all nodes from the merged network that were analyzed for enrichment of cellular processes (GO term annotations) using the BiNGO plugin in Cytoscape. Cellular processes that are significantly enriched and that are linked to cell growth and proliferation are displayed. (B) HeLa cells were transfected with control siRNA (siControl) or siRNA against Sec16 (siSec16) or Sar1A (siSar1A). After 24 h or 48 h, cells were detached and counted using a counting chamber. The results are presented as the fold increase in the number of cells relative to that plated at time-point 0 (t0). The results show the mean±s.d. (C) HeLa cells were transfected with control siRNA or siRNA against Sec16, or treated with 5 μg/ml brefeldin A (BFA) overnight. Lysates were immunoblotted for caspase-3. The upper panel shows a representative experiment, and the lower panel shows an evaluation of three independent experiments depicting the percentage of cleaved versus total caspase-3 as the mean±s.d. (D) HeLa cells were transfected with empty vector (control) or wild-type Ras (RasWT). At 24 h after transfection, cells were lysed and immunoblotted for the indicated proteins. Shown are representative blots from three independent experiments. (E) HeLa cells were transfected with control siRNA or siRNA against Egr1 and Egr3 (siEgr1+3). After 24 h, cells were transfected with plasmid encoding GFP (GFP), wild-type GFP–Sec16 (Sec16-wt), Sec16-Maddin (Maddin), the phosphorylation-deficient Sec16-T415I or Sar1A. At 48 h after transfection, cells were detached and counted using a counting chamber. The results are presented as the fold increase in the number of cells compared with that plated at time-point 0 (t0) and show the mean±s.d. *$P<0.05$ (ANOVA with Tukey's post-hoc test).

endogenous wild-type Sec16. We propose that this is the reason why these mutants themselves induce proliferation, although significantly less than overexpressing wild-type Sec16. We could not test the overexpression of Sec16 variants in cells depleted of endogenous Sec16 because Sec16 silenced cells did not tolerate the overexpression of any plasmid. To test whether any regulator of ER export would behave similarly, we depleted Sar1A and found that it reduced proliferation (Fig. 8B). However, overexpression of Sar1A had no detectable effect on proliferation (Fig. 8E). Taken together, our findings support the notion that ER export and cell proliferation are linked, and we propose that Sec16 is the molecular integrator of these two processes.

DISCUSSION

The integration of metabolic and signaling networks into the secretory pathway remains poorly understood. In the current work, we demonstrated how Sec16 acts as an integrator of growth factor signaling into ERES. We propose that Sec16 is part of a CFFL that functions as a persistence detector for increasing secretory flux upon mitogen signaling. Transient growth factor stimulation increases ERES number, but does not affect the

Journal of Cell Science (2015) 128, 670–682 doi:10.1242/jcs.157115

output (i.e. secretion) on a short timescale. This rapid increase in ERES number is predicted by our modeling to happen at the expense of ERES size. Although the number of ERES is rapidly increasing to be able to cope with an upcoming wave of secretory cargo, they only acquire an appropriate size at longer time scales. Concomitant with an increase in cargo load, Sec16 levels are increased (in a manner dependent on Egr1 and Egr3) to compensate for the reduced size of ERES, rendering ERES fully capable to deal with a higher secretory flux after a few hours. How is Sec16 regulated by Egr1 and Egr3? We did not perform a promoter dissection to test whether these transcription factors bind to the Sec16 promoter. Sec16 expression might also be regulated through mechanisms other than direct promoter control. For instance, Sec16 mRNA could be stored and released upon changes in growth factor levels. However, we did not observe evidence for storage granule formation under serum starvation. Another possibility is that Sec16 could be regulated by miRNAs. For instance, miR-212 and miR-132 have been shown to be regulated by Egr family transcription factors (Wang et al., 2010) and, according to our database search, we found that Sec16 is regulated by these miRNAs (www.genecards.org).

Sec16 was shown to bind to ERES through an arginine-rich region without major help from co-factors (Ivan et al., 2008). Others have shown that Sec16 remains associated with ERES throughout mitosis without the presence of COPII (Hughes et al., 2009). Therefore, it was proposed that Sec16 is able to cluster at domains of the ER and to form a ‘template’ for the biogenesis of ERES that acts independently of COPII components. However, it remains unclear how this template function is mediated and how and whether it is regulated dynamically. Although this template model might be correct in the context of mitotic disassembly and reassembly of ERES, we propose that the situation is more dynamic in the context of an adaptive response of ERES to growth factor signaling. The fact that Sec16-Maddin that is unable to bind to Sec23 did not respond to growth factor treatment indicates that the adaptive response to growth factors (i.e. the rapid increase in ERES number) requires an interaction of Sec16 with COPII. Once recruited to the ERES, Sec16 would then act to stabilize COPII on ERES, for instance, reducing the rate of GTP hydrolysis of Sar1 (Kung et al., 2012). Unlike other more static interpretations, our model of an adjustable mutual stabilization of Sec16 and COPII components is capable of including a dynamic cellular response while remaining fully compatible with key features of the steady state of the cell, e.g. a strict COPII-dependent emergence of a secretory flux. Although this study focused the role of mitogens in regulating ERES, others have recently identified in *Drosophila* a novel response of ERES to amino acid starvation (Zacharogianni et al., 2014), which is distinct from the response to serum starvation reported previously (Zacharogianni et al., 2011). Amino acid starvation results in the formation of ‘Sec bodies’, where Sec16 and other COPII components are stored. These structures form in a manner dependent on Sec24AB and Sec16, illustrating a cooperation between Sec16 and COPII components in the response to stress. This is analogous to our findings that also show that the binary interaction of Sec16 with COPII is essential for ERES to properly respond to alterations in growth factor levels.

Our findings also indicate that Sec16 (or secretion in general) is relevant for the ability of cells to proliferate. Based on this, we are tempted to speculate that Sec16 expression is linked to conditions of deregulated cellular proliferation such as cancer. Indeed, such a conclusion is facilitated by a recent screen of the proteome of eight colon cancer patients comparing healthy colonic tissue with the diseased tissue. Sec16 was found to be upregulated approximately twofold in colonic cancer samples compared with its expression in healthy tissue (Wiśniewski et al., 2012). This was not due to general upregulation of all secretory pathway components, as ERGIC-53 was downregulated (Wiśniewski et al., 2012), which is in agreement with earlier reports on the link between ERGIC-53 and cancer (Roeckel et al., 2009). Our findings demonstrate that changes in the number of ERES are part of the cellular response to mitogen treatment and therefore imply a close link between the regulation of secretion and cell growth and proliferation. An integrative view on the secretory pathway becomes even more important when aiming at deconvolving the results of recent systems biology approaches that have identified numerous signaling, metabolic or transcriptional regulators that have an effect on the secretory pathway at various levels (Bard et al., 2006; Farhan et al., 2010; Kondylis et al., 2011; Simpson et al., 2012; Chia et al., 2012).

MATERIALS AND METHODS

Fluorescence recovery after photobleaching

FRAP was performed with a LeicaSP5 confocal microscope using a 63×/1.4 NA oil-immersion objective at fivefold digital magnification. All experiments were performed at 37℃. Glass coverslips were transferred to a Ludin chamber (Life Imaging Services GmbH) and covered with imaging medium (DMEM supplemented with 20 mM HEPES pH 7.4). After acquisition of a pre-bleach image, the ERES was bleached at 100% laser intensity for 750 ms. After bleaching, images were acquired at one image per second. Images were analyzed using ImageJ. For fitting FRAP curves, we used the reaction-dominated single-exponential recovery that has been widely used in the literature (Sprague et al., 2006). The mobile fraction was calculated as $q=(F_\infty-F_0)/(F_i-F_0)$, where F_∞ is fluorescence in the bleached region after recovery, F_i is the fluorescence in the bleached region before bleaching, and F_0 is the fluorescence in the bleached region directly after bleaching.

ERES quantification

ERES were quantified in cells immunostained for Sec16 or Sec31 or in cells expressing GFP–Sec16. Images were acquired using a LeicaSP5 confocal microscope, with a 63×/1.4 NA oil-immersion objective at threefold digital magnification. ERES were quantified using ImageJ by applying uniform thresholding to the images to exclude non-specific structures. Structures smaller than 2 pixels in size were excluded from analysis as these typically represented noise originating from image pixelization. In the case of GFP–Sec16-expressing cells, total fluorescence intensity of cells was measured, and ERES were only quantified from cells displaying comparable fluorescence intensity (within a twofold intensity range), thereby excluding possible effects due to the grade of GFP–Sec16 overexpression.

Regulatory sequence analysis

We used the PRIMA algorithm (Elkon et al., 2003) to scan the 500-bp region upstream of the transcription start site for enriched binding sites. Enrichment was calculated with respect to similar 500-bp regions upstream of transcription start sites for the entire genome. This analysis revealed 184 enriched matrices corresponding to 180 transcription factors. We further scored each enriched transcription factor according to its shortest distance in a protein–protein interaction network from either EGFR or IGF1R and ranked the transcription factors accordingly. Sequences and annotations for the regions, based on Human Genome build 19, were downloaded from EMBL on 30 August 2012. Transcription factor binding sites, represented as position weight matrices were downloaded from TRANSFAC (Matys et al., 2006) database release 11.1. A protein–protein interaction network was taken from ANAT (Yosef et al., 2011).

Fluorescence correlation spectroscopy

FCS measurements were performed on a Leica SP5 SMD system equipped with a custom-made climate chamber for 37°C incubation. Samples were illuminated at 488 nm through a water-immersion objective (HCX PL APO 63× 1.2W CORR), fluorescence detection used a bandpass filter (500–530 nm). The pinhole was set to one Airy unit. FCS data were fitted using the fitting function for two non-interacting populations with normal diffusion:

$$C(\tau)=\frac{fA}{\left(1+\tau/\tau_{\mathrm{D}}^{(1)}\right)}+\frac{(1-f)A}{\left(1+\tau/\tau_{\mathrm{D}}^{(2)}\right)}$$

The first term with amplitude f and diffusion time $\tau_{\mathrm{D}}^{(1)}=r_0^2/(4\mathrm{D_c})$ describes a fast diffusing species, e.g. cytosolic Sec16–GFP, whereas the second term with amplitude $(1-f)$ and diffusion time $\tau_{\mathrm{D}}^{(2)}=r_0^2/(4\mathrm{D_m})$ describes a slow diffusing species, e.g. membrane-bound Sec16–GFP. Both diffusion times are determined by the radius of the confocal volume, $r_0\approx220$nm, and the respective diffusion constants, $\mathrm{D_c}$ and $\mathrm{D_m}$. For simplicity, we have neglected a factor $\sqrt{\left(1+\tau/(S^2\tau_{\mathrm{D}}^{(2)})\right)}$ in the denominator of the first summand. This factor captures diffusion along the optical axis, yet owing to the unavoidable elongation of the confocal volume (described by $S^2\approx25$) it had little influence on the fit parameters reported here. The prefactor A is proportional to the inverse number of GFP-tagged Sec16 molecules in the focus (here typically 20–100) and it also encodes the photophysics of GFP on timescales of ~10 µs. Because all diffusion times were well beyond 300 µs, the contribution of photophysics to A was negligible for the fitting process. Autocorrelation curves were collected for 60 s in regions of the peripheral ER, i.e. away from the nuclear rim, for several loci in a variety of cells and treatments. FCS curves were fitted individually, and the mean of the obtained diffusion coefficients (24 curves for untreated cells; 16 for starved and mitogen-treated cells) are reported in the main text.

Theoretical predictions for diffusion constants of Sec16 in cytosol and on membranes were derived as follows. We assumed Sec16 to be globular with a mass about 10-fold larger than GFP and a hydrodynamic radius ~2.2-fold larger than GFP, i.e. $R=3.3$ nm. Based on the Einstein–Stokes equation $D=k_BT/(6\pi\eta R)$ the diffusion constant is $\mathrm{D_c}=17$ µm^2/s. We used a cytosolic viscosity η 4-fold larger than that of water (Elsner et al., 2003); $\mathrm{k_BT}$ is thermal energy. For the diffusion of Sec16 on membranes, we employed the Saffman–Delbruck relation for peripheral membrane proteins (Morozova et al., 2011), from which one infers a diffusion constant of Sec16 in the gross range of $\mathrm{D_m}=1$ µm^2/s.

Acknowledgements

M.W. would like to thank H. Brandt and W. Zimmermann for helpful discussions on phase separation scenarios.

Competing interests

The authors declare no competing or financial interests.

Author contributions

M.W. and H.F. conceived the study, analyzed data and wrote the manuscript. K.D.T. performed experiments, analyzed data and wrote the manuscript. V.R., F.B., J.H., V.M. and M.A.H. performed experiments and analyzed data. D.F.L. contributed reagents. A.M., N.A. and R.S. performed bioinformatic analyses.

Funding

H.F. is supported by a grant from the Swiss National Science Foundation (SNF) and by a R'Equipe grant from the SNF; by the Young Scholar Fund of the University of Konstanz; by the German Science Foundation; and by the Canton of Thurgau. J.H. and M.W. acknowledge support from the Deutsch-Israelische Projektkooperation [grant number GA 309/10-1]; Deutsche Forschungsgemeinschaft [grant number WE4335/2-1]; and Human Frontier Science Program [grant number RGY0076/2010].

Supplementary material

Supplementary material available online at
http://jcs.biologists.org/lookup/suppl/doi:10.1242/jcs.157115/-/DC1

References

Bard, F., Casano, L., Mallabiabarrena, A., Wallace, E., Saito, K., Kitayama, H., Guizzunti, G., Hu, Y., Wendler, F., Dasgupta, R. et al. (2006). Functional genomics reveals genes involved in protein secretion and Golgi organization. *Nature* **439**, 604-607.

Bhattacharyya, D. and Glick, B. S. (2007). Two mammalian Sec16 homologues have nonredundant functions in endoplasmic reticulum (ER) export and transitional ER organization. *Mol. Biol. Cell* **18**, 839-849.

Boncompain, G., Divoux, S., Gareil, N., de Forges, H., Lescure, A., Latreche, L., Mercanti, V., Jollivet, F., Raposo, G. and Perez, F. (2012). Synchronization of secretory protein traffic in populations of cells. *Nat. Methods* **9**, 493-498.

Buchan, J. R., Kolaitis, R. M., Taylor, J. P. and Parker, R. (2013). Eukaryotic stress granules are cleared by autophagy and Cdc48/VCP function. *Cell* **153**, 1461-1474.

Budnik, A. and Stephens, D. J. (2009). ER exit sites—localization and control of COPII vesicle formation. *FEBS Lett.* **583**, 3796-3803.

Chia, J., Goh, G., Racine, V., Ng, S., Kumar, P. and Bard, F. (2012). RNAi screening reveals a large signaling network controlling the Golgi apparatus in human cells. *Mol. Syst. Biol.* **8**, 629.

Connerly, P. L., Esaki, M., Montegna, E. A., Strongin, D. E., Levi, S., Soderholm, J. and Glick, B. S. (2005). Sec16 is a determinant of transitional ER organization. *Curr. Biol.* **15**, 1439-1447.

Dudognon, P., Maeder-Garavaglia, C., Carpentier, J. L. and Paccaud, J. P. (2004). Regulation of a COPII component by cytosolic O-glycosylation during mitosis. *FEBS Lett.* **561**, 44-50.

Elkon, R., Linhart, C., Sharan, R., Shamir, R. and Shiloh, Y. (2003). Genome-wide in silico identification of transcriptional regulators controlling the cell cycle in human cells. *Genome Res.* **13**, 773-780.

Elsner, M., Hashimoto, H., Simpson, J. C., Cassel, D., Nilsson, T. and Weiss, M. (2003). Spatiotemporal dynamics of the COPI vesicle machinery. *EMBO Rep.* **4**, 1000-1004.

Espenshade, P., Gimeno, R. E., Holzmacher, E., Teung, P. and Kaiser, C. A. (1995). Yeast SEC16 gene encodes a multidomain vesicle coat protein that interacts with Sec23p. *J. Cell Biol.* **131**, 311-324.

Farhan, H., Weiss, M., Tani, K., Kaufman, R. J. and Hauri, H.-P. (2008). Adaptation of endoplasmic reticulum exit sites to acute and chronic increases in cargo load. *EMBO J.* **27**, 2043-2054.

Farhan, H., Wendeler, M. W., Mitrovic, S., Fava, E., Silberberg, Y., Sharan, R., Zerial, M. and Hauri, H.-P. (2010). MAPK signaling to the early secretory pathway revealed by kinase/phosphatase functional screening. *J. Cell Biol.* **189**, 997-1011.

Forster, R., Weiss, M., Zimmermann, T., Reynaud, E. G., Verissimo, F., Stephens, D. J. and Pepperkok, R. (2006). Secretory cargo regulates the turnover of COPII subunits at single ER exit sites. *Curr. Biol.* **16**, 173-179.

Fowler, T., Sen, R. and Roy, A. L. (2011). Regulation of primary response genes. *Mol. Cell* **44**, 348-360.

Gedde, U. W. (1995). *Polymer Physics*. Dordrecht: Kluwer Academic Publishers.

Gimeno, R. E., Espenshade, P. and Kaiser, C. A. (1996). COPII coat subunit interactions: Sec24p and Sec23p bind to adjacent regions of Sec16p. *Mol. Biol. Cell* **7**, 1815-1823.

Guo, Y. and Linstedt, A. D. (2006). COPII-Golgi protein interactions regulate COPII coat assembly and Golgi size. *J. Cell Biol.* **174**, 53-63.

Heinzer, S., Wörz, S., Kalla, C., Rohr, K. and Weiss, M. (2008). A model for the self-organization of exit sites in the endoplasmic reticulum. *J. Cell Sci.* **121**, 55-64.

Hughes, H., Budnik, A., Schmidt, K., Palmer, K. J., Mantell, J., Noakes, C., Johnson, A., Carter, D. A., Verkade, P., Watson, P. et al. (2009). Organisation of human ER-exit sites: requirements for the localisation of Sec16 to transitional ER. *J. Cell Sci.* **122**, 2924-2934.

Ivan, V., de Voer, G., Xanthakis, D., Spoorendonk, K. M., Kondylis, V. and Rabouille, C. (2008). Drosophila Sec16 mediates the biogenesis of tER sites upstream of Sar1 through an arginine-rich motif. *Mol. Biol. Cell* **19**, 4352-4365.

Jin, L., Pahuja, K. B., Wickliffe, K. E., Gorur, A., Baumgärtel, C., Schekman, R. and Rape, M. (2012). Ubiquitin-dependent regulation of COPII coat size and function. *Nature* **482**, 495-500.

Kondylis, V., Tang, Y., Fuchs, F., Boutros, M. and Rabouille, C. (2011). Identification of ER proteins involved in the functional organisation of the early secretory pathway in Drosophila cells by a targeted RNAi screen. *PLoS ONE* **6**, e17173.

Koreishi, M., Yu, S., Oda, M., Honjo, Y. and Satoh, A. (2013). CK2 phosphorylates Sec31 and regulates ER-To-Golgi trafficking. *PLoS ONE* **8**, e54382.

Kung, L. F., Pagant, S., Futai, E., D'Arcangelo, J. G., Buchanan, R., Dittmar, J. C., Reid, R. J., Rothstein, R., Hamamoto, S., Snapp, E. L. et al. (2012). Sec24p and Sec16p cooperate to regulate the GTP cycle of the COPII coat. *EMBO J.* **31**, 1014-1027.

Lee, K. C., Siegel, J., Webb, S. E., Lévêque-Fort, S., Cole, M. J., Jones, R., Dowling, K., Lever, M. J. and French, P. M. (2001). Application of the stretched exponential function to fluorescence lifetime imaging. *Biophys. J.* **81**, 1265-1274.

Lee, M. C., Miller, E. A., Goldberg, J., Orci, L. and Schekman, R. (2004). Bi-directional protein transport between the ER and Golgi. *Annu. Rev. Cell Dev. Biol.* **20**, 87-123.

Lim, W. A., Lee, C. M. and Tang, C. (2013). Design principles of regulatory networks: searching for the molecular algorithms of the cell. *Mol. Cell* **49**, 202-212.

Lord, C., Bhandari, D., Menon, S., Ghassemian, M., Nycz, D., Hay, J., Ghosh, P. and Ferro-Novick, S. (2011). Sequential interactions with Sec23 control the direction of vesicle traffic. *Nature* **473**, 181-186.
Matys, V., Kel-Margoulis, O. V., Fricke, E., Liebich, I., Land, S., Barre-Dirrie, A., Reuter, I., Chekmenev, D., Krull, M., Hornischer, K. et al. (2006). TRANSFAC and its module TRANSCompel: transcriptional gene regulation in eukaryotes. *Nucleic Acids Res.* **34**, D108-D110.
Montegna, E. A., Bhave, M., Liu, Y., Bhattacharyya, D. and Glick, B. S. (2012). Sec12 binds to Sec16 at transitional ER sites. *PLoS ONE* **7**, e31156.
Morozova, D., Guigas, G. and Weiss, M. (2011). Dynamic structure formation of peripheral membrane proteins. *PLOS Comput. Biol.* **7**, e1002067.
Nyfeler, B., Reiterer, V., Wendeler, M. W., Stefan, E., Zhang, B., Michnick, S. W. and Hauri, H. P. (2008). Identification of ERGIC-53 as an intracellular transport receptor of alpha1-antitrypsin. *J. Cell Biol.* **180**, 705-712.
Reiterer, V., Nyfeler, B. and Hauri, H. P. (2010). Role of the lectin VIP36 in post-ER quality control of human alpha1-antitrypsin. *Traffic* **11**, 1044-1055.
Roeckel, N., Woerner, S. M., Kloor, M., Yuan, Y. P., Patsos, G., Gromes, R., Kopitz, J. and Gebert, J. (2009). High frequency of LMAN1 abnormalities in colorectal tumors with microsatellite instability. *Cancer Res.* **69**, 292-299.
Sharpe, L. J., Luu, W. and Brown, A. J. (2011). Akt phosphorylates Sec24: new clues into the regulation of ER-to-Golgi trafficking. *Traffic* **12**, 19-27.
Shaywitz, D. A., Espenshade, P. J., Gimeno, R. E. and Kaiser, C. A. (1997). COPII subunit interactions in the assembly of the vesicle coat. *J. Biol. Chem.* **272**, 25413-25416.
Shen-Orr, S. S., Milo, R., Mangan, S. and Alon, U. (2002). Network motifs in the transcriptional regulation network of Escherichia coli. *Nat. Genet.* **31**, 64-68.
Simpson, J. C., Joggerst, B., Laketa, V., Verissimo, F., Cetin, C., Erfle, H., Bexiga, M. G., Singan, V. R., Hériché, J. K., Neumann, B. et al. (2012). Genome-wide RNAi screening identifies human proteins with a regulatory function in the early secretory pathway. *Nat. Cell Biol.* **14**, 764-774.
Sprague, B. L., Müller, F., Pego, R. L., Bungay, P. M., Stavreva, D. A. and McNally, J. G. (2006). Analysis of binding at a single spatially localized cluster of binding sites by fluorescence recovery after photobleaching. *Biophys. J.* **91**, 1169-1191.
Sukhatme, V. P. (1990). Early transcriptional events in cell growth: the Egr family. *J. Am. Soc. Nephrol.* **1**, 859-866.
Supek, F., Madden, D. T., Hamamoto, S., Orci, L. and Schekman, R. (2002). Sec16p potentiates the action of COPII proteins to bud transport vesicles. *J. Cell Biol.* **158**, 1029-1038.
Wang, W., Zhou, D., Shi, X., Tang, C., Xie, X., Tu, J., Ge, Q. and Lu, Z. (2010). Global Egr1-miRNAs binding analysis in PMA-induced K562 cells using ChIP-Seq. *J. Biomed. Biotechnol.* **2010**, 867517.
Watson, P., Townley, A. K., Koka, P., Palmer, K. J. and Stephens, D. J. (2006). Sec16 defines endoplasmic reticulum exit sites and is required for secretory cargo export in mammalian cells. *Traffic* **7**, 1678-1687.
Whittle, J. R. and Schwartz, T. U. (2010). Structure of the Sec13-Sec16 edge element, a template for assembly of the COPII vesicle coat. *J. Cell Biol.* **190**, 347-361.
Wiśniewski, J. R., Ostasiewicz, P., Duś, K., Zielińska, D. F., Gnad, F. and Mann, M. (2012). Extensive quantitative remodeling of the proteome between normal colon tissue and adenocarcinoma. *Mol. Syst. Biol.* **8**, 611.
Yosef, N., Zalckvar, E., Rubinstein, A. D., Homilius, M., Atias, N., Vardi, L., Berman, I., Zur, H., Kimchi, A., Ruppin, E. et al. (2011). ANAT: a tool for constructing and analyzing functional protein networks. *Sci. Signal.* **4**, pl1.
Zacharogianni, M., Kondylis, V., Tang, Y., Farhan, H., Xanthakis, D., Fuchs, F., Boutros, M. and Rabouille, C. (2011). ERK7 is a negative regulator of protein secretion in response to amino-acid starvation by modulating Sec16 membrane association. *EMBO J.* **30**, 3684-3700.
Zacharogianni, M., Aguilera Gomez, A., Veenendaal, T., Smout, J. and Rabouille, C. (2014). A reversible non-membrane bound stress assembly that confers cell viability by preserving ERES components during amino-acid starvation. *eLife* **3**, 4132.
Zanetti, G., Pahuja, K. B., Studer, S., Shim, S. and Schekman, R. (2012). COPII and the regulation of protein sorting in mammals. *Nat. Cell Biol.* **14**, 20-28.

Journal of Cell Science